

oxidation of the alkyl-substituted carbyne complexes **3** and **4** is achieved at $-95\text{ }^\circ\text{C}$. The initially dark red solutions turn orange brown upon warming to room temperature. The products are recrystallized¹⁸ from CH_2Cl_2 /pentane and obtained as dark green **7**¹⁵ and dark turquoise **8**¹⁶ microcrystals in 70% and 50% yield, respectively. The new alkylidyne complexes **5-8** are thermally stable but very sensitive toward the atmosphere.

With the oxidation reaction described in this paper and the methods developed earlier^{9,10} thermally stable carbyne complexes of both known types of the group 6¹⁷ transition metals are now easily accessible. The *trans*-halotetracarbonylmetal carbyne complexes, while rather thermally labile themselves,⁷ prove to be the critical intermediates in these synthetic procedures.

Acknowledgment. This work was supported by the National Science Foundation (CHE-8411023) and by the donors of the Petroleum Research Fund, administered by the American Chemical Society.

(14) **4**: Chromatography on silica at $-40\text{ }^\circ\text{C}$, eluted with pentane/ CH_2Cl_2 , 5:2. ¹³C NMR (CDCl_3 , $-40\text{ }^\circ\text{C}$) δ 293.9 ($J_{\text{CW}} = 172.3\text{ Hz}$, CCH_2CMe_3), 192.1 ($J_{\text{CW}} = 129.1\text{ Hz}$, CO).

(15) **7**: Anal. Calcd for $\text{C}_6\text{H}_{13}\text{Br}_2\text{O}_2\text{W}$: C, 13.33; H, 2.42; Br, 44.33. Found: C, 13.34; H, 2.33; Br, 45.99. ¹H NMR (CD_2Cl_2) δ 7.32 (s, 3, $^3J_{\text{WH}} = 9.8\text{ Hz}$, CCH_3); ¹³C NMR (CD_2Cl_2 , $-20\text{ }^\circ\text{C}$) δ 337.5 ($J_{\text{CW}} = 219\text{ Hz}$, CMe).

(16) **8**: Anal. Calcd for $\text{C}_{10}\text{H}_{21}\text{Br}_2\text{O}_2\text{W}$: C, 20.12; H, 3.55. Found: C, 20.14; H, 3.77. ¹H NMR (CD_2Cl_2) δ 7.41 (s, 2, $^3J_{\text{WH}} = 7\text{ Hz}$, CCH_2CMe_3); ¹³C NMR (CDCl_3 , $-20\text{ }^\circ\text{C}$) δ 345.4 ($J_{\text{CW}} = 215\text{ Hz}$, CCH_2CMe_3).

(17) In this paper the periodic group notation is in accord with recent actions by IUPAC and ACS nomenclature committees. A and B notation is eliminated because of wide confusion. Groups IA and IIA become groups 1 and 2. The d-transition elements comprise groups 3 through 12, and the p-block elements comprise groups 13 through 18. (Note that the former Roman number designation is preserved in the last digit of the new numbering: e.g., III \rightarrow 3 and 13.)

(18) After removal of the solvent from the reaction solution the dark orange-brown solid is taken up in a small amount of CH_2Cl_2 (typically 5 mL of CH_2Cl_2 per mmol of product) and precipitated with pentane (3 \times to 4 \times the volume of CH_2Cl_2 present). This precipitation procedure is repeated two or three times. The resulting solid (orange-brown, **5**; deep green, **6-8**) is taken up in a small amount of CH_2Cl_2 , cooled to $0\text{ }^\circ\text{C}$, and filtered to remove any insolubles. Pentane is added to the resulting solution to precipitate the product as a microcrystalline powder. For R = alkyl the initial precipitate is removed as well by filtration when it is oily.

Zirconoxycarbene Complexes of Ruthenium—Reduction of Coordinated CO in the Reaction of a Zr–Ru Compound with H_2

Charles P. Casey* and Robert E. Palermo

Department of Chemistry, University of Wisconsin
Madison, Wisconsin 53706

Arnold L. Rheingold*

Department of Chemistry, University of Delaware
Newark, Delaware 19711

Received September 6, 1985

We have synthesized compounds with directly bonded early and late transition metals such as $\text{Cp}_2\text{Zr}[\text{Ru}(\text{CO})_2\text{Cp}]_2$ (**1**) in the hope of cleaving the metal–metal bond with H_2 .¹ The resulting mixture containing reactive hydridic M–H and acidic M–H units might be a powerful reducing system for polar molecules including CO. Here we present evidence for a circuitous stepwise conversion of **1** into Ru–H and Zr–H units and for the reduction of coordinated CO to a formyl or zirconoxy carbene group.

Previously, we reported that **1** reacts with ethylene or with CO to form the strained, reactive adducts **2** or **3** and to expel

(1) Casey, C. P.; Jordan, R. F.; Rheingold, A. L. *Organometallics* **1984**, *3*, 504.

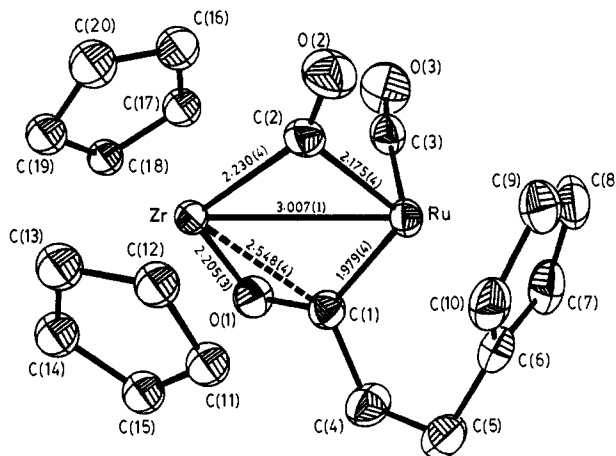
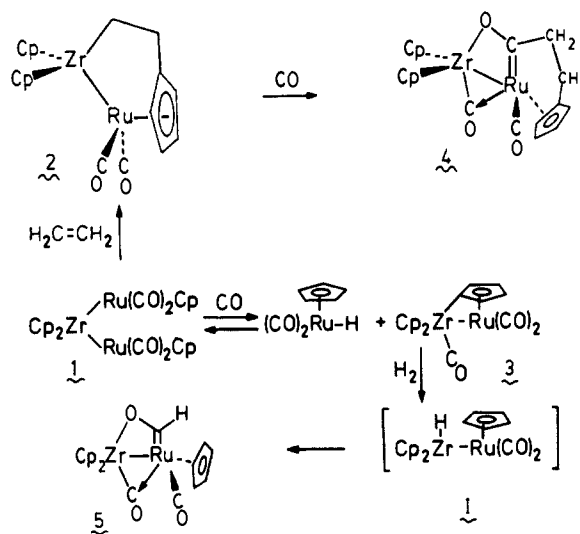


Figure 1. Molecular structure and labeling scheme for **4**.

$\text{CpRu}(\text{CO})_2\text{H}$.² Here we report that the reaction of **2** with CO and the reaction of **3** with H_2 produce zirconoxycarbene complexes of ruthenium.



When an amber C_6D_6 solution of ethylene product **2** was treated with CO (700 mm), the solution slowly turned dark red. ¹H NMR demonstrated that **2** was converted to **4** without the intervention of a detectable intermediate ($t_{1/2} \approx 15\text{ h}$). Crystalline **4** was isolated in 80% yield from the reaction of **2** with CO (760 mm) in toluene at $55\text{ }^\circ\text{C}$ for 30 h. The structure of **4** was determined by single-crystal X-ray diffraction (Figure 1).³

The metals in **4** are linked by a direct Zr–Ru bond (3.007 Å), by a zirconoxycarbene bound to Ru (which can also be regarded as a Zr-complexed Ru–acyl), and by a semibridging carbonyl bound strongly to Zr. The metrical details of this semibridging carbonyl are similar to those in $\text{Cp}_2\text{Zr}(\text{CO})(\mu\text{-}\eta^1(\text{Zr}),\eta^5\text{-C}_5\text{H}_4\text{-Ru}(\text{PMe}_3)(\text{CO}))$.²

The key spectral features of **4** which characterize its structural type are the ¹³C NMR and IR parameters associated with the carbonyl ligands and the zirconoxycarbene ligand.⁴ In the ¹³C NMR of **4**, the terminal ruthenium CO appears at δ 205, the semibridging CO appears at δ 316, and the carbene carbon appears at δ 279 as a peak significantly broadened by unresolved two-bond

(2) Casey, C. P.; Palermo, R. E.; Jordan, R. F.; Rheingold, A. L. *J. Am. Chem. Soc.* **1985**, *107*, 4597.

(3) See the supplementary material for details of X-ray crystallography.

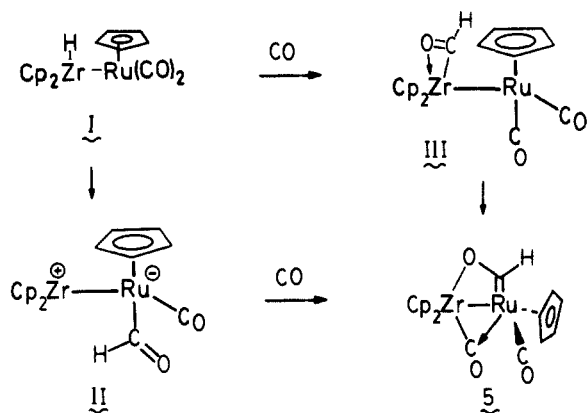
(4) ¹H NMR (benzene- d_6) δ 5.71 (s, 5 H, CpZr), 5.62 (m, 1 H, C_5H_4), 5.06 (s, 5 H, CpZr), 4.94 (m, 1 H, C_5H_4), 4.81 (m, 1 H, C_5H_4) 4.35 (m, 1 H, C_5H_4), 3.62 (dt, $J = 18, 8\text{ Hz}$, 1 H, $\text{C}(\text{O})\text{CHH}$), 2.92 (ddd, $J = 18, 8, 4\text{ Hz}$, 1 H, $\text{C}(\text{O})\text{CHH}$), 1.75 (ddd, $J = 14, 10, 4\text{ Hz}$, 1 H, $\text{C}(\text{O})\text{CH}_2\text{CHH}$), 1.42 (dt, $J = 12, 9\text{ Hz}$, 1 H, $\text{C}(\text{O})\text{CH}_2\text{CHH}$). ¹³C{¹H} NMR (THF- d_6 , $26\text{ }^\circ\text{C}$) δ 316 ($\mu\text{-CO}$), 279 (ZrOC=Ru), 205 (RuCO), 127 (C, of C_5H_4), 108 (CpZr), 105 (CpZr), 104 (CH_2), 92, 89, 84, 79 (C_5H_4), 22 (CH_2).

coupling to the α -methylene protons. In the IR spectrum of **4**, bands were observed at 1909 cm^{-1} for the terminal CO, at 1704 cm^{-1} for the semibridging CO, and at 1380 cm^{-1} for the C-O stretch of the zirconoxycarbene.

When the reaction of **2** with ^{13}C was monitored by ^{13}C NMR, the isotopic label initially appeared only at the carbene carbon of **4**. This observation is consistent with initial insertion of CO into the Zr-CH₂ bond, to form an η^2 -acyl zirconium intermediate, followed by rapid transfer of the very electrophilic η^2 -acyl carbon to the electron-rich ruthenium. Such acyl transfers have been observed before in Zr/Mo systems⁵ and may be a general phenomenon in early/late heterobimetallic compounds.

When the CO product **3** was reacted with H₂ (700 mm) at room temperature in THF, the hydrido-zirconoxycarbene complex **5** was obtained ($t_{1/2} \approx 40$ min). No intermediates were observed by ^1H NMR in THF-*d*₈. The structure of **5** is very similar to that of **4** and was established by spectroscopy. **5** does not possess a plane of symmetry and consequently three Cp resonances are seen in the ^1H NMR at δ 5.78, 5.40, and 5.39. The ruthenium-bound Cp ligand arises from hydrogenolysis of the Zr-C₅H₄ bond. The hydrogen attached to the Ru-bound zirconoxycarbene carbon (or Zr complexed ruthenium formyl) appears at δ 14.05. The IR spectrum of **5** has bands at 1930 cm^{-1} for the terminal Ru-CO, at 1740 cm^{-1} for the semibridging Zr-CO, and at 1350 cm^{-1} for the C-O stretch of the zirconoxy carbene unit. The correspondence between the IR spectra of **4** and **5** indicates that these complexes have the same functional groups. **5** has only limited stability in solution and decomposes slowly at room temperature to a complex mixture of products. **5** was isolated as a slightly impure red solid that slowly decomposes at ambient temperature.

Earlier ^{13}C exchange studies on **3** demonstrated that rapid CO dissociation from Zr occurs to generate a reactive intermediate² which has a Zr-based orbital available for interaction with H₂. We suggest that reaction of this intermediate with H₂ leads to hydrogenolysis of the strained Zr-C₅H₄ bond and formation of zirconium hydride intermediate I. This strained Zr-C₅H₄ bond is also cleaved by Cp(CO)₂RuH² and by *t*-BuOH,⁶ hydrogenolysis of Zr-C bonds has been observed previously.⁷ There are two plausible routes from I to **5**. First, addition of the Zr-H to a ruthenium carbonyl⁸ could produce ruthenium formyl complex II which could readd CO to Zr to produce **5**. Alternatively, CO



could coordinate to I at Zr and insert into the Zr-H bond to produce the η^2 -formyl zirconium complex III. Formyl migration to ruthenium as suggested for the formation of **4** could produce

(5) Longato, B.; Norton, J. R.; Huffman, J. C.; Marsella, J. A.; Caulton, K. G. *J. Am. Chem. Soc.* **1981**, *103*, 209. Marsella, J. A.; Huffman, J. C.; Caulton, K. G.; Longato, B.; Norton, J. R. *J. Am. Chem. Soc.* **1982**, *104*, 6360.

(6) Casey, C. P.; Palermo, R. E., unpublished results.

(7) Gell, K. I.; Schwartz, J. *J. Am. Chem. Soc.* **1978**, *100*, 3246.

(8) Intermolecular addition of a zirconium hydride to coordinated CO has been reported. Threlkel, R. S.; Bercaw, J. E. *J. Am. Chem. Soc.* **1981**, *103*, 2650. Wolczanski, P. T.; Threlkel, R. S.; Bercaw, J. E. *J. Am. Chem. Soc.* **1979**, *101*, 218. Barger, P. T.; Bercaw, J. E. *Organometallics*, **1984**, *3*, 278. Barger, P. T.; Santarsiero, B. D.; Armantrout, J.; Bercaw, J. E. *J. Am. Chem. Soc.* **1984**, *106*, 5178.

5. Studies utilizing selectively labeled **3** are in progress to distinguish these alternatives.

It should be noted that reaction of $\text{Cp}_2\text{Zr}[\text{Ru}(\text{CO})_2\text{Cp}]_2$ (**1**) with CO and then with H₂ resulted in a net cleavage of a Zr-Ru bond by H₂ and in the formation of the late-transition-metal hydride $\text{Cp}(\text{CO})_2\text{RuH}$ and of the early-transition-metal hydride intermediate $\text{Cp}_2\text{Zr}(\text{H})\text{Ru}(\text{CO})_2\text{Cp}$ (**I**).

Acknowledgment. Support from the Department of Energy, Division of Basic Energy Sciences, is gratefully acknowledged.

Supplementary Material Available: X-ray crystal data for **4** (28 pages). Ordering information is given on any current masthead page.

Molecular Orbital Calculations on the Th-Ni Interaction in $\text{Th}(\eta^5\text{-C}_5\text{H}_5)_2(\mu\text{-PH}_2)_2\text{Ni}(\text{CO})_2$

J. V. Ortiz

Department of Chemistry, University of New Mexico
Albuquerque, New Mexico 87131

Received September 10, 1985

Organometallic chemists continue to search for new types of bonding and the relatively unexplored chemistry of the f-block elements¹ presents inviting possibilities. Stimulated by the recent observation² of a short Th-Ni separation in $\text{Th}(\eta^5\text{-C}_5(\text{CH}_3)_5)_2(\mu\text{-PPh}_2)_2\text{Ni}(\text{CO})_2$, the following extended Hückel³ calculations seek to clarify the nature of the proposed metal-metal interaction.

If one considers the central ThP₂Ni quadrilateral (Figure 1) with the average observed Th-P and Ni-P bond lengths, it is possible to vary the Th-Ni distance by changing the Th-P-Ni angle. (*C*_{2v} symmetry is maintained in these calculations on $\text{Th}(\eta^5\text{-C}_5\text{H}_5)_2(\mu\text{-PH}_2)_2\text{Ni}(\text{CO})_2$; the structures of the $(\text{C}_5\text{H}_5)_2\text{Th}$ and $\text{Ni}(\text{CO})_2$ fragments are also held constant.) Two structural extremes are now defined. The first has the experimental Th-Ni separation of 3.206 Å while the second takes 3.70 Å for the same quantity. This latter figure arises from an ionic model assumption in which metal atom radii are summed.² Th-P-Ni angles range from 76° to 93° and the P-P distance from 3.84 to 3.41 Å as the Th-Ni separation is increased.

At first glance, the plot of reduced atomic overlap populations (see Figure 2) for this distortion seems disappointing, since the Th-Ni values are negative.⁴ Yet the trend with respect to metal-metal separation is encouraging. Of all the interactions, this one changes the most. Note the relative passivity of Th-P overlap population; apparently there is some geometrical flexibility about the Th-Ni bonding with P is at a maximum when the P-Ni-P angle is near 110°. Of course, P-P overlap populations are indicative of lone pair repulsions and grow more negative as the P-P distance decreases.

Now let the molecule be divided into two fragments: $\text{Cp}_2\text{Th}(\text{PH}_2)_2$ and $\text{Ni}(\text{CO})_2$. In terms of the molecular orbitals of these entities, two principal sources of Th-Ni interaction are discernible. First is the filled-filled repulsion between the d-levels of the Ni

(1) (a) Marks, T. J. *Science (Washington, D.C.)* **1982**, *217*, 989-997. (b) Marks, T. J., Fischer, R. D., Eds. "Organometallics of the f-Elements"; D. Reidel: Dordrecht, 1979. (c) Watson, P. L.; Parshall, G. W. *Acc. Chem. Res.* **1985**, *18*, 51-56. (d) Evans, W. J. *J. Organomet. Chem.* **1983**, *250*, 217-226.

(2) Ritchey, J. M.; Zozulin, A. J.; Wroblewski, D. A.; Ryan, R. R.; Wasserman, H. J.; Moody, D. C.; Paine, R. T. *J. Am. Chem. Soc.* **1985**, *107*, 501-503.

(3) (a) Hoffmann, R. *J. Chem. Phys.* **1963**, *39*, 1397-1412. (b) Hoffmann, R.; Lipscomb, W. N. *Ibid.* **1962**, *36*, 2179-2195; **1962**, *37*, 2872-2883. (c) Weighted *H_{ij}* formulae are employed here: Ammeter, J. H.; Burgi, H. B.; Thibeault, J. C.; Hoffmann, R. *J. Am. Chem. Soc.* **1978**, *100*, 3686-3692. (d) Th *H_{ii}* (in eV): -27.07 (6p), -5.99 (5f), -4.95 (6d), -5.31 (7s), -3.22 (7p). Slater exponents and contraction coefficients: 3.43 6p; 5.154 (0.5679), 2.468 (0.5936) 5f; 2.756 (0.5789), 1.441 (0.5717) 6d; 1.742 7s; 2.5 (-1.3102), 2.0 (2.035) 7p. The 7p basis function is orthogonal to the 6p basis function.

(4) Reduced atomic overlap populations are indices of the degree of bonding between two atoms. Negative values imply a net antibonding relationship.